Malaysian Journal of Mathematical Science 6(1): 75-96 (2012)

Numerical Simulation for the Viscous Flow inside Complex Shapes Using Grid Generation

Saleh M. Al-Harbi

Department of Mathematics, Universal College in Makkah, Umm Al-Qura University, Makkah, Saudi Arabia

E-mail: salharbi434@yahoo.com

ABSTRACT

In this paper, we determined a numerical solution of the incompressible Navier-stokes equation in the vorticity-stream function formulation. The solution is based on a technique of elliptic grid generation in which we transform the physical domain into rectangular computational domain, which requires the use of a curvilinear coordinate system to transform the governing equations to be applied on the computational domain. The transformed equations are approximated using central differences and solved simultaneously by the Alternating Direction Implicit method and successive-over relaxation iteration method.

Keywords: Alternating direction implicit method, successive over relaxation iteration method, Navier-Stokes equation.

1. INTRODUCTION

In many engineering applications, lubrication, channel flows, pipe flows, the contraction appears frequently, which makes it necessary to study thoroughly the distribution of the streamlines and their values along the geometry of the flow with different contraction ratio Costas *et al.* (1998). Ismaiel *et al.* (2003) determined a numerical solution for the incomprssible Navier Stokes equations for the flow inside contraction geometry using elliptic grid generation technique. Salem (2004) and Salem (2006) studied the incomprssible Navier Stokes equations for the flow inside contraction geometry using different numerical techniques. In this paper we will impose some assumption on the mathematical model, which appears in the physical case on the irregular-shapes (Peyret and Taylor (1983)). We produce the numerical solution, of the two-dimensional Navier-Stokes equations in a non-orthogonal curvilinear coordinate system. That can treat the method of automatic numerical generation of a general curvilinear coordinate system coordinate lines coincident with all boundaries of a simply connected region (Liseikin (1999) and Kmupp and Stanly (1994)).

The curvilinear coordinates being generated as the solutions of two elliptic partial differential equations (Thompson (1985)). Regardless of the shape and number of bodies and regardless of the spacing of the curvilinear coordinate lines, all numerical computation, both to generate the coordinate system and to subsequently solve the Navier-Stokes equations on the coordinate system, is done on the rectangular grid with square mesh, which is the computational plane. We apply the numerical grid generation technique to find a numerical solution of the two dimensional, incompressible viscous flow equations written in the vorticity-stream function formulation on contraction geometry. The computational plane is a rectangular shape, which is divided into an equally spaced grid system. The transformed equations of the governing equations are approximated by finite difference formulation, which is solved in the rectangular grid system.

2. TRANSFORMATIONS OF PARTIAL DIFFERENTIAL EQUATINS

In order to overcome the problem of the physical domain, we use the method of grid generation in which we transform the physical domain into rectangular computational domain (Hoffman (1989) and Middelecoff and Thomas(1980)). Now, it is required to perform all numerical computations in the uniform rectangular transformed plane, in order to do that, the dependent and independent variables interchanged. Define the following relations between the physical and computational spaces in Figure 1.

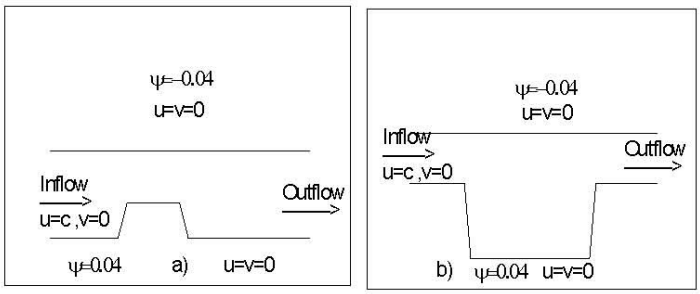

Figure 1: The physical geometry with boundary conditions

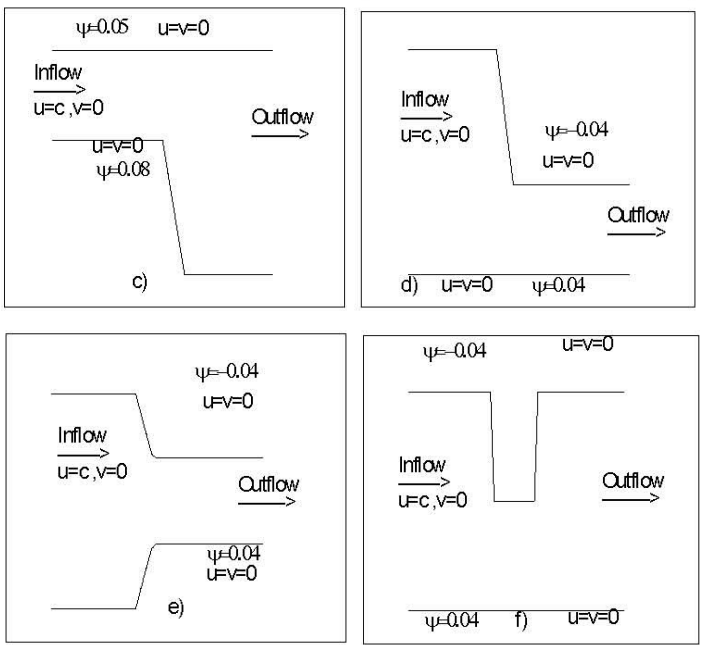

Figure 1 (continued): The physical geometry with boundary conditions

Two-dimensional elliptic boundary value problems are considered. The general transformation from the physical plane (x, y) to the transformed plane (ξ, η) is

$$\xi = \xi(x, y),$$

$$\eta = \eta(x, y) \tag{2.1}$$

and

$$\xi_x = \frac{y_\eta}{J},$$

$$\xi_y = -\frac{x_\eta}{J},$$

$$\eta_x = -\frac{y_\xi}{J},$$

$$\eta_y = \frac{x_\xi}{J}, \tag{2.2}$$

where

$$J = J\left[\frac{x, y}{\xi, \eta}\right] = x_\xi y_\eta - x_\eta y_\xi. \tag{2.3}$$

Now, for any function f, the first derivative in the computational domain is given by

$$\frac{\partial f}{\partial x} = \left(\frac{1}{J}\right)\left[y_\eta f_\xi - y_\xi f_\eta\right],$$

$$\frac{\partial f}{\partial y} = \left(\frac{1}{J}\right)\left[x_\xi f_\eta - x_\eta f_\xi\right], \tag{2.4}$$

and the Laplaceian is defined as:

$$\nabla^2 f = \left(\frac{1}{J^2}\right)\left(\alpha f_{\xi\xi} - 2\beta f_{\xi\eta} + \gamma f_{\eta\eta} + \sigma f_\eta + \tau f_\xi\right), \tag{2.5}$$

where

$$\begin{aligned}
\alpha &= x_\eta^2 + y_\eta^2, \\
\beta &= x_\xi x_\eta + y_\xi y_\eta, \\
\gamma &= y_\xi^2 + y_\xi^2, \\
\sigma &= \left(\frac{1}{J}\right)\left[y_\xi A - x_\xi B\right], \\
\tau &= \left(\frac{1}{J}\right)\left[x_\eta B - y_\eta A\right],
\end{aligned} \tag{2.6}$$

and

$$A = \alpha x\xi\xi - 2\beta x_{\xi\eta} + \gamma x_{\eta\eta}, \tag{2.7}$$

$$B = \alpha y\xi\xi - 2\beta y_{\xi\eta} + \gamma y_{\eta\eta}. \tag{2.8}$$

The transformation of the time derivative from physical domain to computational domain takes the form:

$$\left(\frac{\partial f}{\partial t}\right)_{x,y} = \frac{\partial(x,y,f)}{\partial(\xi,\eta,t)} \Big/ \frac{\partial(x,y,t)}{\partial(\xi,\eta,t)},$$

$$\frac{\partial(x,y,t)}{\partial(\xi,\eta,t)} = \begin{bmatrix} x_\xi & x_\eta & x_t \\ y_\xi & y_\eta & y_t \\ 0 & 0 & 1 \end{bmatrix} = x_\xi y_\eta - x_\eta y_\xi, \tag{2.9}$$

$$\begin{aligned} \frac{\partial(x,y,t)}{\partial(\xi,\eta,t)} &= \begin{bmatrix} x_\xi & x_\eta & x_t \\ y_\xi & y_\eta & y_t \\ f_\xi & f_\eta & f_t \end{bmatrix} \\ &= x_\xi\left(y_\eta f_t - y_t f_\eta\right) - x_\eta\left(y_\xi f_t - y_t f_\xi\right) + x_t\left(y_\xi f_\eta - y_\eta f_\xi\right) \\ &= \left(x_\xi y_\eta - x_\eta y_\xi\right) f_t + \left(x_\eta f_\xi - x_\xi f_\eta\right) y_t + \left(y_\xi f_\eta - y_\eta f_\xi\right) x_t. \end{aligned} \tag{2.10}$$

Finally, the time derivative in the computational domain takes the form:

$$\left(\frac{\partial f}{\partial t}\right)_{x,y} = \left(\frac{\partial f}{\partial t}\right)_{\xi,\eta} + \left(\frac{1}{J}\right)\left[y_\xi f_\eta - y_\eta f_\xi\right] x_t + \left(\frac{1}{J}\right)\left[x_\eta f_\xi - x_\xi f_\eta\right] y_t.$$

The system of elliptic equations:

$$\alpha x_{\xi\xi} - 2\beta x_{\xi\eta} + \gamma x_{\eta\eta} = 0,$$

$$\alpha y_{\xi\xi} - 2\beta y_{\xi\eta} + \gamma y_{\eta\eta} = 0. \tag{2.11}$$

Its solved in the computational domain (ξ,η) in order to provide the grid point locations in the physical space (x,y) in the general case can be conveniently solved by the finite-difference method with the successive over relaxation (SOR) method Smith (1985) of the dependent variables and under relaxation of the coefficients with linearly interpolated initial guess Barfield (1970); Yanenko (1971)). The values of the coefficients α,β,γ and J are stored for use in the solution of the partial differential equations.

The grid system on the physical and computational planes is shown in Figure 2 for the six contractions respectively.

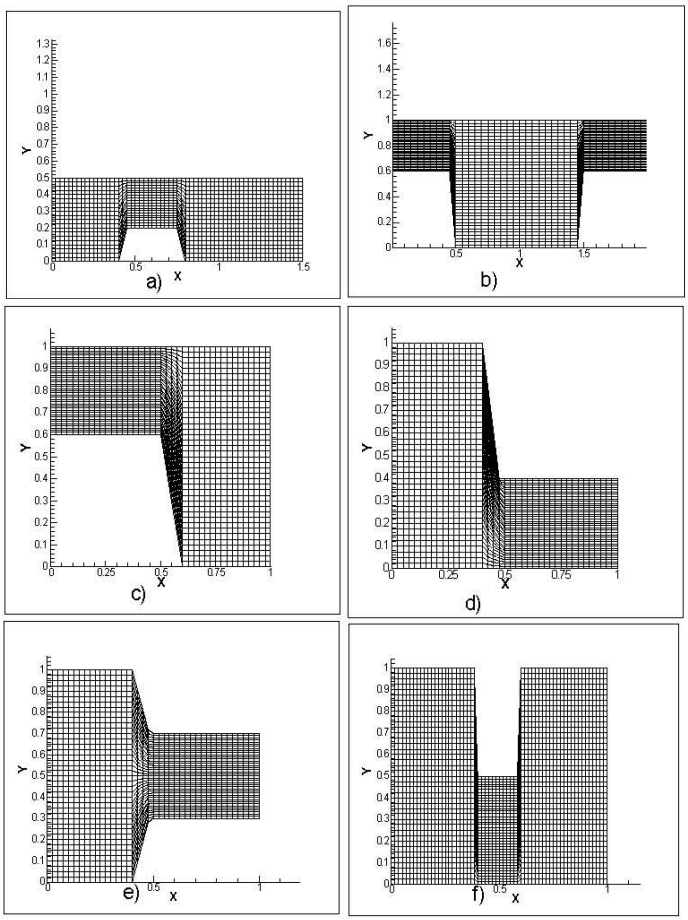

Figure 2: Grid system on the physical plane for contraction geometry

3. FORMULATION OF THE PROBLEM

The differential equations governing the motion of an incompressible viscous fluid inside a back step, T-shape, high dam-shape, L-shape, nozzle, U-shape are the two-dimensional stream-vorticity formulation (Cheng and Tser (1991)). These equations are

$$\omega_t + u\omega_x + \upsilon\omega_y = \frac{1}{\mathrm{Re}}\nabla^2\omega, \tag{3.1}$$

$$\nabla^2\psi = -\omega. \tag{3.2}$$

Where u, υ are the velocity components of the flow, *Re* is the Reynolds number, ψ is the steam function, ω is the vorticity and $\nabla^2(\ ) = \frac{\partial^2(\ )}{\partial x^2} + \frac{\partial^2(\ )}{\partial y^2}$. The velocity components are calculated from the equations

$$u = \psi_y, \qquad \upsilon = -\psi_x. \tag{3.3}$$

4. NUMERICAL SOLUTION USING GRID GENERATION TECHNIQUE

To obtain the numerical solution using grid generation technique, we transform the governing Equations (3.1) and (3.2) from the physical domain into the computational domain. The non-conservative form is chosen here,

$$\omega_t = \left[\omega_t\right]_{\zeta,\eta} - \left(\omega_x x_t + \omega_y y_t\right). \tag{4.1}$$

For steady case $x_t = y_t = 0,$ therefore

$$\omega_t = \left[\omega_t\right]_{\zeta,\eta}, \tag{4.2}$$

$$\omega_x = \frac{1}{J} - \left(y_\eta\omega_\xi - y_\xi\omega_\eta\right), \tag{4.3}$$

$$\omega_y = \frac{1}{J}\left(x_\xi\omega_\eta - x_\eta\omega_\xi\right), \tag{4.4}$$

$$\psi_x = \frac{1}{J}\left(y_\eta\psi_\xi - y_\xi\psi_\eta\right), \tag{4.5}$$

$$\psi_y = \frac{1}{J}\left(x_\xi \psi_\eta - x_\eta \psi_\xi\right), \tag{4.6}$$

$$\nabla^2 \omega = \frac{1}{J^2}\left(\alpha\omega_{\xi\xi} - 2\beta\omega_{\xi\eta} + \gamma\omega_{\eta\eta} + \sigma\omega_\eta + \tau\omega_\xi\right), \tag{4.7}$$

$$\nabla^2 \psi = \frac{1}{J^2}\left(\alpha\psi_{\xi\xi} - 2\beta\psi_{\xi\eta} + \gamma\psi_{\eta\eta} + \sigma\psi_\eta + \tau\psi_\xi\right), \tag{4.8}$$

$$\upsilon_x = \frac{1}{J}\left(y_\eta \upsilon_\xi - y_\xi \upsilon_\eta\right), \tag{4.9}$$

$$u_y = \frac{1}{J}\left(x_\xi u_\eta - x_\eta u_\xi\right). \tag{4.10}$$

According to the relations (2.4) to (2.11) the giving equations (3.1) and (3.2) are transformed to the computational plane as

$$\begin{aligned} &\omega_t + \frac{u}{J}\left(y_\eta \omega_\xi - y_\xi \omega_\eta\right) + \frac{\upsilon}{J}\left(x_\xi \omega_\eta - x_\eta \omega_\xi\right) \\ &= \frac{1}{J^2 Re}\left(\alpha\omega_{\xi\xi} - 2\beta\omega_{\xi\eta} + \gamma\omega_{\eta\eta} + \sigma\omega_\eta + \tau\omega_\xi\right), \end{aligned} \tag{4.11}$$

$$\frac{1}{J^2}\left(\alpha\psi_{\xi\xi} - 2\beta\psi_{\xi\eta} + \gamma\psi_{\eta\eta} + \sigma\psi_\eta + \tau\psi_\xi\right) = -\omega, \tag{4.12}$$

where α, β, γ are functions of ξ and η, which are defined in Equation (2.6), σ and τ are given by

$$\sigma = \frac{1}{J}\left[y_\xi\left(\alpha x_{\xi\xi} - 2\beta x_{\xi\eta} + \gamma x_{\eta\eta}\right) - x_\xi\left(\alpha y_{\xi\xi} - 2\beta y_{\xi\eta} + \gamma y_{\eta\eta}\right)\right], \tag{4.13}$$

$$\tau = \frac{1}{J}\left[x_\eta\left(\alpha y_{\xi\xi} - 2\beta y_{\xi\eta} + \gamma y_{\eta\eta}\right) - y_\eta\left(\alpha x_{\xi\xi} - 2\beta x_{\xi\eta} + \gamma x_{\eta\eta}\right)\right]. \tag{4.14}$$

The transformed equations of the velocity components are

$$u = \frac{1}{J}\left(x_\xi \psi_\eta - x_\eta \psi_\xi\right), \tag{4.15}$$

$$\upsilon = \frac{-1}{J}\left(y_\eta \psi_\xi - y_\xi \psi_\eta \right). \tag{4.16}$$

5. NUMERICAL SOLUTION USING FINITE DIFFERENCE METHOD

The giving equations are applied at every interior grid point on the discrete grid system (including the re-entrant boundaries and all derivatives Thames *et al.* (1977) and Smith and Leschziner (1995)). To obtain the FDE of Equation (4.11), we use the alternating direction implicit (ADI) method which have two steps given by:

Step 1: We rearrange Equation (4.11) as

$$\begin{aligned} &\omega_t + \frac{1}{J}\left(uy_\eta - vx_\eta - \frac{\tau}{JRe} \right)\omega_\xi - \frac{\alpha}{J^2 Re}\omega_{\zeta\zeta} \\ &= \frac{1}{J}\left(uy_\zeta - \upsilon x_\zeta - \frac{\sigma}{JRe} \right)\omega_\eta + \frac{1}{J^2 Re}\left(\gamma\omega_{\eta\eta} - 2\beta\varpi_{\xi\eta} \right). \end{aligned} \tag{5.1}$$

Then the finite difference approximation of this equation given by

$$\begin{aligned} &\left[1 + \frac{\Delta t}{2}\left[\frac{1}{J_{i,j}}\left(u_{i,j}^n \left(y_\eta \right)_{i,j} - \upsilon_{i,j}^n \left(x_\eta \right)_{i,j} - \frac{\tau_{i,j}}{J_{i,j} Re} \right)\frac{\Theta_\zeta}{2\Delta_\zeta} - \frac{\alpha_{i,j}}{J_{i,j}^2 Re}\Theta_{\zeta\zeta} \right] \right] \omega_{i,j}^{n+\frac{1}{2}} \\ &= \left[1 + \frac{\Delta t}{2}\left[\frac{1}{J_{i,j}}\left(u_{i,j}^n \left(y_\zeta \right)_{i,j} - \upsilon_{i,j}^n \left(x_\zeta \right)_{i,j} - \frac{\sigma_{i,j}}{J_{i,j} Re} \right)\frac{\Theta_\eta}{2\Delta_\eta} \right] \right] \omega_{i,j}^n \\ &\quad + \frac{\Delta t}{2J_{i,j}^2 Re}\left[\gamma_{i,j}\Theta_{\eta\eta} - 2\beta_{i,j}\Theta_{\xi\eta} \right]\omega_{i,j}^n. \end{aligned} \tag{5.2}$$

Step 2: We rearrange equation (4.11) as

$$\begin{aligned} &\omega_t + \frac{1}{J}\left(\upsilon x_\zeta - u\ y_\zeta - \frac{\sigma}{JRe} \right)\omega_\eta - \frac{\gamma}{J^2 Re}\omega_{\eta\eta} \\ &= \frac{1}{J}\left(\upsilon x_\eta - u\ y_\eta - \frac{\tau}{JRe} \right)\omega_\zeta + \frac{1}{J^2 Re}\left(\alpha\omega_{\zeta\zeta} - 2\beta\omega_{\zeta\eta} \right). \end{aligned} \tag{5.3}$$

Then the finite difference approximation of this equation given by

$$\left[1+\frac{\Delta t}{2}\left[\frac{1}{J_{i,j}}\left(\upsilon_{i,j}^{n}\left(x_{\zeta}\right)_{i,j}-u_{i,j}^{n}\left(y_{\zeta}\right)_{i,j}-\frac{\sigma_{i,j}}{J_{i,j}R_{e}}\right)\frac{\Theta_{\eta}}{2\Delta_{\eta}}-\frac{\gamma_{i,j}}{J_{i,j}^{2}R_{e}}\Theta_{\eta\eta}\right]\right]\omega_{i,j}^{n+1}$$
$$=\left[1+\frac{\Delta t}{2}\left[\frac{1}{J_{i,j}}\left(\upsilon_{i,j}^{n}\left(x_{\eta}\right)_{i,j}-u_{i,j}^{n}\left(y_{\eta}\right)_{i,j}+\frac{\tau_{i,j}}{J_{i,j}R_{e}}\right)\frac{\Theta_{\zeta}}{2\Delta\zeta}\right]\right]\omega_{i,j}^{n+\frac{1}{2}} \qquad (5.4)$$
$$+\frac{\Delta t}{2J_{i,j}^{2}R_{e}}\left[\alpha_{i,j}\Theta_{\zeta\zeta}-2\beta_{i,j}\Theta_{\xi\eta}\right]\omega_{i,j}^{n+\frac{1}{2}}$$

where

$$\Theta_{\zeta\omega_{i,j}^{n}}=\omega_{i+1,j}^{(n)}-\omega_{i-1,j}^{n}$$
$$\Theta_{\eta}\omega_{i,j}^{n}=\omega_{i+1,j}^{(n)}-\omega_{i,j-1}^{(n)}$$
$$\Theta_{\zeta\zeta}\omega_{i,j}^{n}=\frac{\omega_{i+1,j}^{(n)}-2\omega_{i,j}^{n}+\omega_{i-1,j}^{(n)}}{\left(\Delta\zeta\right)^{2}}$$
$$\Theta_{\eta\eta}\omega_{i,j}^{n}=\frac{\omega_{i,j+1}^{(n)}-2\omega_{i,j}^{n}+\omega_{i,j+1}^{(n)}}{\left(\Delta\eta\right)^{2}}$$
$$\Theta_{\zeta\eta}\omega_{i,j}^{n}=\frac{\omega_{i+1,j+1}^{n}+\omega_{i-1,j-1}^{(n)}-\omega_{i-1,j+1}^{(n)}-\omega_{i+1,j-1}^{(n)}}{4\Delta\zeta\Delta\eta}. \qquad (5.5)$$

Now, we know from Equations (5.2) and (5.4) the solution of $\omega_{i,j}^{n+1}$ at time step $(n+1)$ by using the boundary conditions of ψ and ω. Also the finite difference form of equation (4.12) defined by

$$\frac{1}{J_{i,j}^{2}\left(\nabla\xi\right)^{2}}\left[\alpha_{i,j}\left(\psi_{i+1,j}^{(n+1)}-2\psi_{i,j}^{(n+1)}+\psi_{i-1,j}^{(n+1)}\right)\right]$$
$$\frac{1}{J_{i,j}^{2}\left(\nabla\eta\right)^{2}}\left[\gamma_{i,j}\left(\psi_{i,j+1}^{(n+1)}-2\psi_{i,j}^{(n+1)}+\psi_{i,j-1}^{(n+1)}\right)\right]$$
$$-\frac{1}{4J_{i,j}^{2}\nabla\xi\nabla\eta}\left[2\beta_{i,j}\left(\psi_{i+1,j+1}^{(n+1)}+\psi_{i-1,j-1}^{(n+1)}-\psi_{i+1,j-1}^{(n+1)}-\psi_{i-1,j+1}^{(n+1)}\right)\right]$$
$$+\frac{1}{2J_{i,j}^{2}\nabla\eta}\left[\sigma_{i,j}\left(\psi_{i,j-1}^{(n+1)}\right)\right]+\frac{1}{2J_{i,j}^{2}\nabla\xi}\left[\tau_{i,j}\left(\psi_{i+1,j}^{(n+1)}-\psi_{i-1,j}^{(n+1)}\right)\right]$$
$$=-\omega_{i,j}^{(n+1)}. \qquad (5.6)$$

Where the coefficient $\alpha_{i,j}, \beta_{i,j}, \gamma_{i,j}, \sigma_{i,j}$ and $\tau_{i,j}$ are known from the grid generation system such that when performed $\omega_{i,j}^{(n+1)}$ at time step $(n+1)$, then we shall solve this system (5.6) using SOR.

6. RESULTS AND DISCUSSION

The results or the numerical treatment of the stream function, vorticity and velocity in the contraction geometries as see on Figure 2 and for Reynolds number 50 and 1000 are presented in Figures 3-8.

For the geometry in Figure 2(a) the computed stream function results in different constant-stream lines in Figures 3(a) and 4(a), respectively for two chosen Reynolds numbers. The stream lines are shown at the time in the contraction flow. Many of the features described above are clearly seen including the separation zone in the left lower and right lower kinks.

The stream functions have common features, forming vortex at these places. It is noteworthy that the vortex formed at the contraction is stronger for greater Reynolds number. Also this is in fact physically acceptable because assuming the decrease of visicosity with increasing Reynolds number, the velocity of the fluid increase and consequently the vortex stronger at the contraction. This could be clearly seen from the vorticity patterns in Figures 5(a) and 6(a). We are also show the changes of the velocities with the change of Reynolds number. In Figures 7(a) and 8(a), we show that velocity diagram with changing x at approximately $y = 0.25$.

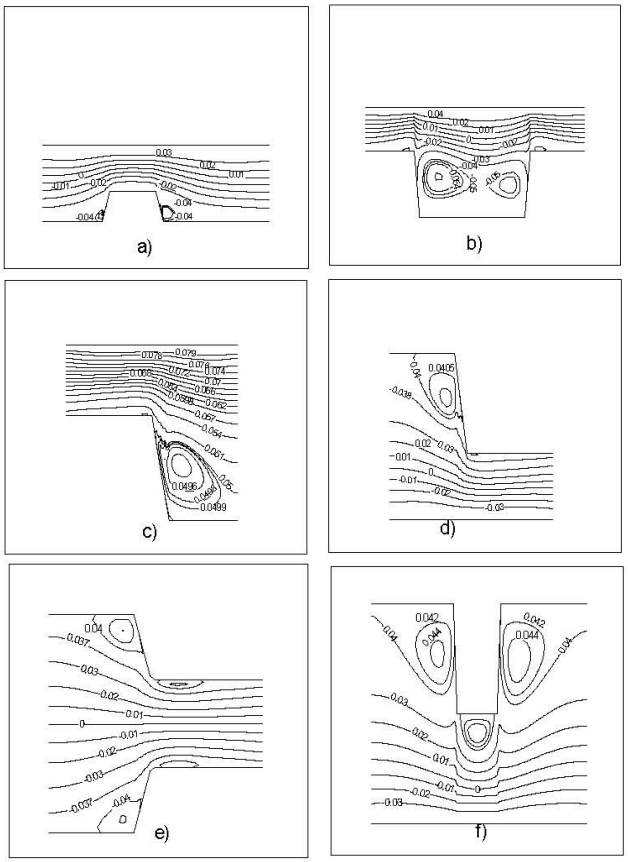

Figure 3: Stream function contours at Re=50

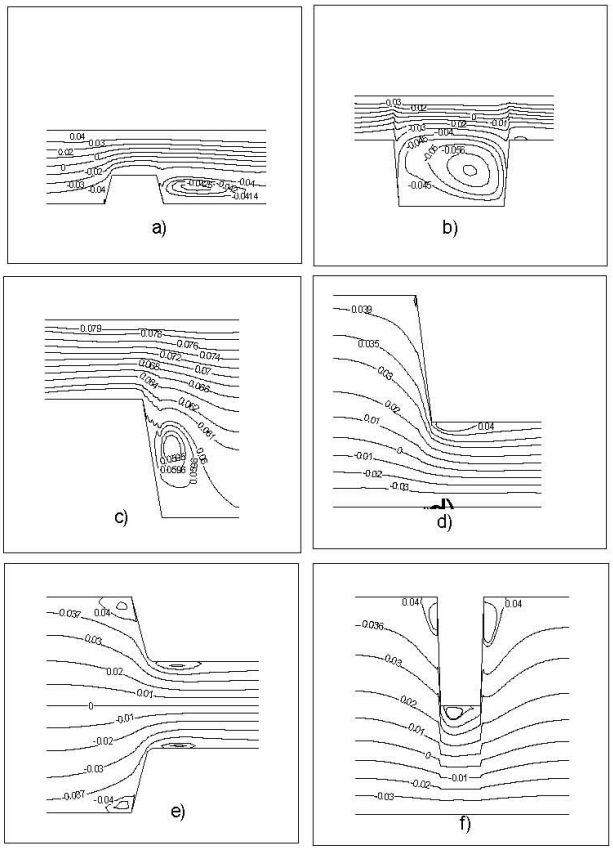

Figure 4: Stream function contours at Re=1000

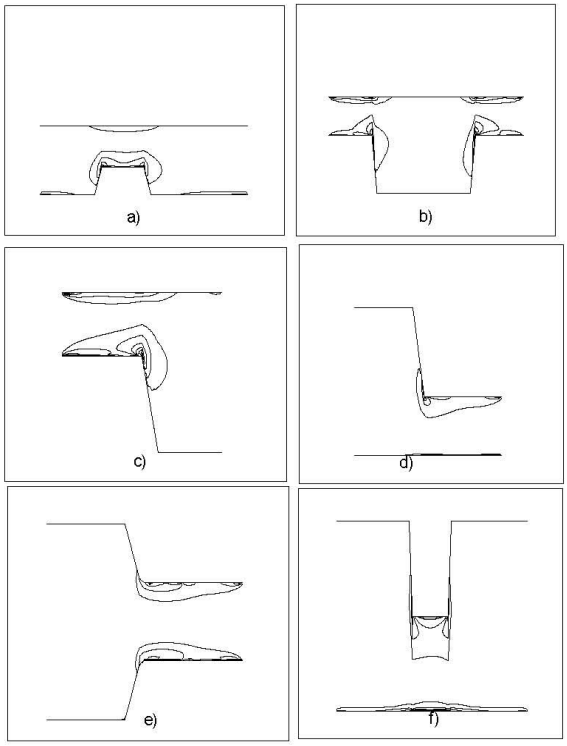

Figure 5: Vorticity contours at Re=50

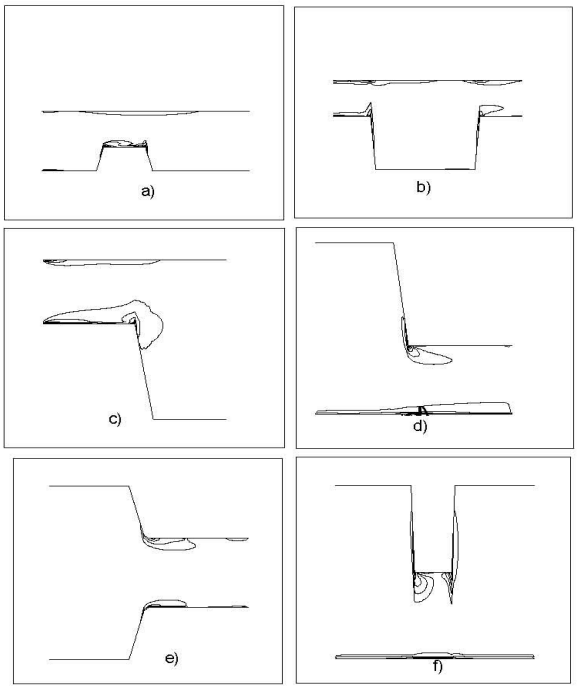

Figure 6: Vorticity contours at Re=1000

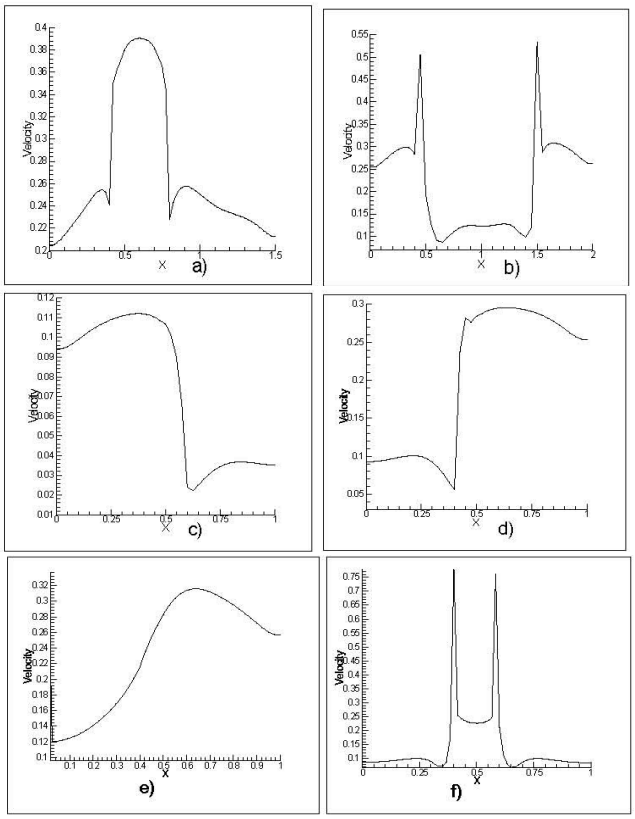

Figure 7: Velocity profiles at Re=50

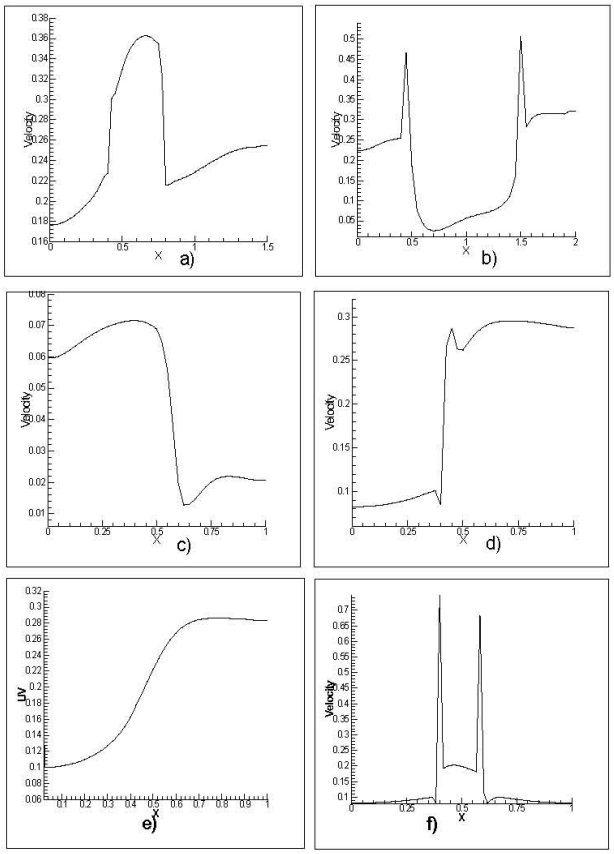

Figure 8: Velocity profiles at Re=1000

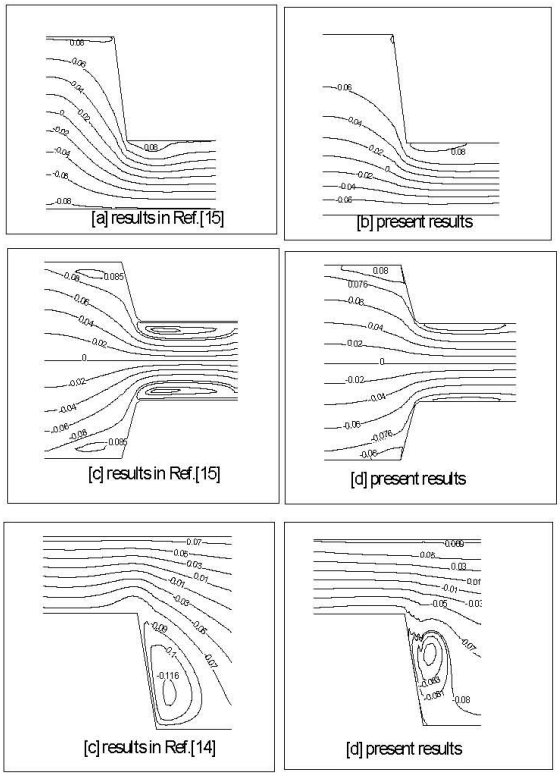

Figure 9: Stream function contours (compared results) at Re=1000

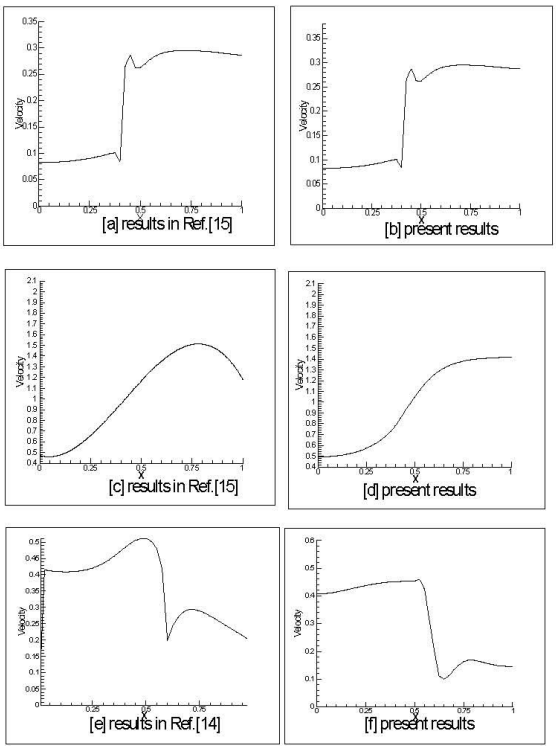

Figure 10: Velocity profiles (compared results) at Re=1000

For the second geometry (T-shape of Figure 2(b)), the results of the computed stream function, Figures 3(b) and 4(b), give different constant-stream lines for two chosen Reynolds numbers. We note that at the left and right lower edges the separation zone increase with increasing Reynolds number. This is also shown by vorticity patterns in Figures 5(b) and 6(b). Another different result for this second geometry is the velocity change at the left and right lower sharpe edges shown in Figures 7(b) and 8(b) with changing x at approximately $y = 0.8,$ we note that at this point the velocity attains maximum.

For the third geometry (high dam-shape of Figure 2(c)), the results of the computed stream functions, Figures 3(c) and 4(c), give the different constant-stream lines for two chosen Reynolds numbers. Here we note that the separation zone in the upstream kink which is the head of the horseshoe vortex, the head of the arch vortex, the reattachment line after that. It is

noteworthy that the vortex formed at the contraction becomes weaker, the increasing Reynolds becomes.

In the fourth geometry (L-shape of Figure 2(d)), the results of the computed stream functions, Figures 3(d) and 4(d), give different constant-stream lines for two chosen Reynolds numbers. We note that there are two singularity points at upper and lower edge. At these points vorticity at upper edge is stronger that the lower. We also note that the vorticity at upper and lower edges becomes weaker with increasing Reynolds number. This could be seen clearly from the vorticity patterns in Figure 5(d) and 6(d). The velocity profiles for this shape at $y = 0.5$ are shown in Figures 7(d) and 8(d).

In the last two geometries ($\vdash$ -shape and $\sqcup$-shape of Figure 2(e) and 2(f)) the results of the computed stream functions Figures 3(e), 3(f) and 4(e), 4(f), give the different constant-stream lines for two chosen Reynolds numbers. We note that the vorticity at singular points are stronger with decreasing Reynolds number. The vorticity contours are shown in Figures 5(e), 5(f) and 6(e), 5(f), whereas the velocity profiles for the last two shapes at $y = 0.5$ are shown in Figures 7(e), 7(f) and 8(e), 8(f).

Finally the computed results are compared with the available results of other investigators, in order to validate the accuracy of the numerical procedure. The stream function contours and velocity profiles are presented together with the results in Figures 10 obtained their results using the vorticity-stream function formulation and using the primitive variable formulation, both studies obtained used grid system for contraction geometry with control function 41x41 grid, all computed results are compared at Reynolds number 1000.

7. CONCLUSION

Within some approximations Reynolds number is inversely proportional to the viscosity of the fluid. Thus, at Re=50 in Figure 4 at high viscosity, some small vortices start to form at singular points for these shapes investigated (Figures 2(a)-2(b)). However, when the Reynolds number increases to Re=1000 (Figures 5(a)-5(b) and 6(a)-6(b)), the vorticity at the contraction becomes weaker when the Reynolds number increases (Figures 5(c)-(f) and 6(c)-6(f)).

REFERENCES

Barfield, W.D. 1970. Numerical method for generating orthogonal curvilinear Meshes. *J Comput. Phys*. **5** (1), 23-33.

Cheng. P. Ping and Tser Son W.U. 1991. Study on the Flow Fields of Irregular-Shaped Domains by an Algebraic Grid Generation Technique. *JSME Int. J., Ser. II*. **34**(1):69-77.

Costas, D., Brian, J.E., Kyung, S.C. and Beris, A.N. 1998. Efficient Pseudospectral Flow Simulations in Moderately Complex Geometries. J. Comput. Phys. **144**: 517-549.

Hoffman, K.A. 1989. *Computational Fluid Dynamics for engineers*. Austin,Texas.

Ismail, I.A., Salem, S.A. and Allan, M.M. 2003. An Elliptic Grid eneration Technique for the Flow Contraction, *Czechoslvak Journal of Physics.* **53**(4): 351-363.

Knupp, P. and Stanly, S. 1994. *Fundamentals of Grid Generation*. CRC Press.

Liseikin,V.D. 1999. *Grid Generation Methods.* Berlin-Heidelberg: Springer-Verlag.

Middelecoff, J.F. and Thomas, P.D. 1980. Direct control of the grid point distribution in meshes generated by elliptic equations. *AIAA. J.* **18**: 652-656.

Peyret, R. and Taylor, T. 1983. *Computational Method for Fluid Flow*. New York: Spring-Verlag.

Salem, S.A. 2004. Numerical simulations for the contraction flow using grid generation. *J. Appl. Math. and Computing*. **16**(1): 383-405.

Salem, S.A. 2006. Study of the contraction flow using grid generation technique. *J. Appl. Math. and Computing*. **21**(1-2): 331-355.

Smith, G.D. 1985. *Numerical solution of Partial Differential Equations*. Oxford: Oxford University Press.

Smith, R.J. and Leschziner, M.A. 1995. Automatic grid-generation for complex geometries, *Aeronautical J*. **2148**:7-14.

Thames, F.C., Thompson, J.F., Mastin C.W. and Walker R.L. 1977, Numerical solutions for viscous and potential flow about arbitrary two dimensional bodies using body-fitted coordinate systems, *J. Comput. Phys*. **24**: 245- 255

Thompson, J. F., Warsi, Z. U. and Mastin, C. W. 1985. *Numerical Grid Generation Foundations and Applications*. North- Holland, New York.

Winslow, A.M. 1967. Numerical solution of the quasilinear Poisson equation in a nonuniform triangle mesh, *J Comput. Phys*. **2**:149-172.

Yanenko, N.N. 1971. *The Method of Fractional Steps*. New York: Springer-Verlag.